Cluster Intensity and Spread Characteristics in Classroom Scenario at 10 and 28 GHz Bands

HANPINITSAK, Panawit; Kentaro, Saito ; Fan, Wei; Hejselbaek, Johannes; Takada, Junichi; Pedersen, Gert Frølund

Published in:
2020 14th European Conference on Antennas and Propagation (EuCAP)

DOI (link to publication from Publisher):
10.23919/EuCAP48036.2020.9135687

Publication date:
2020

Document Version
Accepted author manuscript, peer reviewed version

Cluster Intensity and Spread Characteristics in Classroom Scenario at 10 and 28 GHz Bands

Panawit Hanpinitsak[1], Kentaro Saito[1], Wei Fan[2], Johannes Hejselbaek[3], Jun-ichi Takada[1], Gert Frølund Pedersen[2]
[1]Department of Transdisciplinary Engineering, Tokyo Institute of Technology, Tokyo, Japan
e-mail: hanpinitsak.p@ap.ide.titech.ac.jp, {saitouken,takada}@tse.ens.titech.ac.jp
[2]Department of Electronic Systems, Aalborg University, Aalborg, Denmark
e-mail:{wfa,gfp}@es.aau.dk
[3]Nokia Bell Labs, Aalborg, Denmark
e-mail:joh@ieee.org

***Abstract*—This paper discusses the cluster spreads and scattering intensity (SI) characteristics at 10 and 28 GHz band in a typical classroom environment. The multi-path components (MPCs) were calculated from the measurement data using space-alternating generalized expectation-maximization (SAGE) algorithm. Next, the scattering point-based KPowerMeans (SPKPM) algorithm was used to obtain the clusters based on interacting objects (IOs) in the environment. Lastly, the cluster delay spread (DS), angular spread (AS), and SI were computed and their characteristics were discussed. The results showed that the channels at both bands were almost equally directive. Moreover, cluster spreads depended on the number of layers and surfaces of IOs, whereas IO material and propagation mechanism influenced the cluster SI.**

***Index Terms*—Indoor environments, Millimeter wave propagation, clustering.**

I. Introduction

Because of the increase of data-hungry applications such as augmented reality (AR), virtual reality (VR), and 8K video streaming, the next-generation wireless systems exploiting millimeter wave (mmWave) bands have been deliberated due to the large bandwidth available [1]. Nevertheless, due to higher path-loss and shadowing-loss at these bands, several subbands with large frequency range may be utilized for the future wireless system to combat these issues. Therefore, for system design, it is essential to study the propagation channel characteristics and compare them at different frequency bands.

Consequently, several studies were reported to compare the channel characteristics at different frequency bands in indoor environments. Most of these studies compared angle-delay power spectrum, path-loss, composite delay spread (DS) and angular spread (AS) [2], [3], [4], [5], [6], [7]. Because these measurements were conducted at various types of environments, the channel characteristics may be varied [8] as the propagated waves interact with dissimilar interacting objects (IOs) with different mechanisms. Each IO also consists of a group of diffuse scattering and/or specular paths called cluster.

For that reason, the physical mechanism interpretation of IOs or clusters is crucial to understand and clarify the overall propagation characteristics of each environment. In [9], the cluster power and spread properties were studied at 11 GHz band in a medium-sized hall environment. [10] examined the clusters' major mechanisms at 70 GHz. At 60 GHz, [11] analyzed the cluster reflection loss and gain, and [12] studied the polarimetric cluster gain and spreads. The authors examined the frequency characteristics of scattering intensities (SIs) of clusters from 3 to 28 GHz in a large hall environment with the help of physical optics (PO) [13], and compared the cluster spread characteristics between hall and classroom at 28 GHz [14]. Nonetheless, to the author's best knowledge, the works that discuss the IO level cluster characteristics and compare them at different frequency bands in a small indoor environment such as classroom are still extremely limited in the open literature.

Hence, the cluster spreads and SI characteristics and their comparison between 10 and 28 GHz bands in a typical classroom environment [15], [16] are discussed in this paper. The scattering-point based KPowerMeans (SPKPM) [9], [13] was implemented to acquire the clusters based on the environment geometry. In the next step, cluster AS, DS, and SI were computed and compared among different frequency bands and IOs.

II. Measurement Campaign

The virtual uniform circular array (UCA) channel sounder [2], [17] was used to conduct the measurement. The specifications are shown in Table I. The signal sweep was done by the vector network analyzer (VNA). The commercial biconical antenna [18] was mounted on the transmitter (Tx) and the homemade biconical [19] antenna was put on the receiver (Rx), which was rotated on the robot arm with a 24 cm radius. Tx and Rx were mounted at a height of 1.5 m.

The measurement was conducted in the classroom environment at Aalborg University. Fig. 1 shows the floor plan of the environment. The red-colored words depict the cluster/IO name which will be used to discuss the results in Section IV. Fig. 2 shows photos of each side of the room. The walls are made from plasterboard, which is a multi-layer surface containing metal stud, insulation wool, and plasterboard sheets [20]. There are bookshelves and a projector on the slant plasterboards. The black and whiteboards are located in front

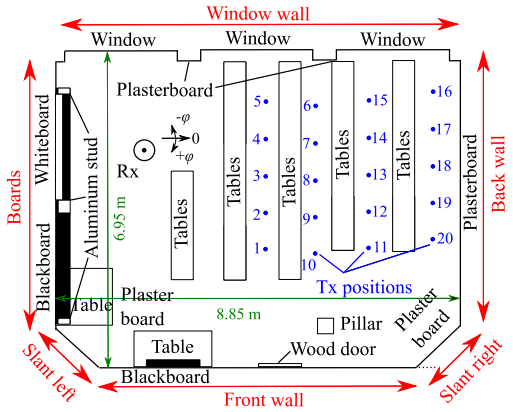

Fig. 1. Measurement floor plan in the classroom environment. *Copyright ©2019 IEICE* [14].

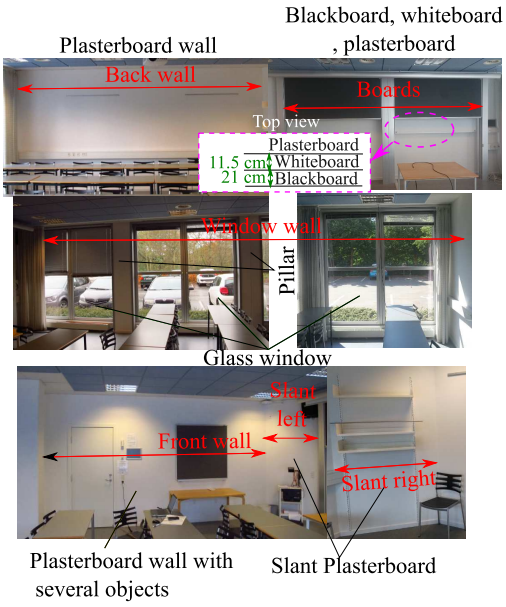

Fig. 2. Photos of each side of room.

of the room. Windows are covered with a thin metallic layer. There are a wood door, small blackboard, and pillar in front of the room. There were 20 Tx spatial snapshots which were spaced 100 cm apart.

TABLE I. Channel sounder specification

Parameters	Values
Center frequency	10 and 28 GHz
Bandwidth	2 GHz
Rx antenna	Modified biconical antenna [19]
Tx antenna	Commercial biconical antenna (A-INFO SZ-2003000) [18]
Radius	0.24 m
Number of Rx elements	360
Height of Tx and Rx	1.5 m

III. Data Analysis Methods

A. Cluster Calculation Methods

The clusters based on the IO geometry were estimated using the algorithm proposed in [13], [14]. After the MPC parameters were estimated from space-alternating generalized expectation-maximization (SAGE) algorithm [21], the measurement-based ray tracer (MBRT) [22] along with the environment map were utilized to obtain the scattering point position in the Cartesian coordinate. Then, the SPKPM [13] was used to obtain the clusters based on the environment geometry.

B. Cluster Spreads and SI Calculation Methods

After the clusters were obtained, the SI, AS, and DS of each cluster were computed. The AS and DS of cluster k were calculated by

$$AS_k = \sqrt{\frac{\sum_{l\in\mathcal{C}_k} P_l \cdot (\phi_l - \bar{\phi}_k)^2}{\sum_{l\in\mathcal{C}_k} P_l}} \tag{1}$$

$$DS_k = \sqrt{\frac{\sum_{l\in\mathcal{C}_k} P_l \cdot (\tau_l - \bar{\tau}_k)^2}{\sum_{l\in\mathcal{C}_k} P_l}} \tag{2}$$

where $\mathcal{C}_k$ is the set of MPCs in cluster k. P_l, ϕ_l, and τ_l are the power, angle-of-arrival (AoA) and delay time (DT) of path l. $\bar{\phi}_k$ and $\bar{\tau}_k$ are the AoA and DT centroids of cluster k, which are calculated by

$$\bar{\phi}_k = \frac{\sum_{l\in\mathcal{C}_k} P_l \cdot \phi_l}{\sum_{l\in\mathcal{C}_k} P_l} \tag{3}$$

$$\bar{\tau}_k = \frac{\sum_{l\in\mathcal{C}_k} P_l \cdot \tau_l}{\sum_{l\in\mathcal{C}_k} P_l} \tag{4}$$

To calculate SI of cluster k, the cluster power P_k is normalized by the free space path gain of the cluster's traveling distance [12].

$$SI_k = P_k - 20\log_{10}\left(\frac{\lambda}{4\pi c\bar{\tau}_k}\right) \tag{5}$$

where c and λ are speed of light and wavelength, respectively.

After the cluster parameters were computed at each Tx position, their mean was calculated over all Tx spatial snapshots.

IV. Results and Discussion

Table. II shows the mean AS, DS, and SI of each cluster. By using SPKPM [13], each cluster is associated with an IO, which corresponds to the red-colored description in Fig. 1. The last row also shows the mean values of all clusters combined.

The results showed that the spreads of IOs with plasterboard as predominant scattering object (Back wall, Front wall, Slant left, and Slant right) were larger than those of Window wall. One possible explanation is that due to the multi-layer structure of the plasterboard and large bandwidth, there were several resolvable MPCs scattered from different layers of plasterboard. In contrast, windows are covered by the metallic-layers, and thus the wave only scattered on the surface. Moreover, the spreads of Boards were much higher than those of other objects because it consists of several flat surfaces with the separation distance of 10-20 cm as shown in Fig. 2. However, since the spreads were mostly small in both bands, the channels of both bands were highly directive. The SIs of Boards and Window were large due to scattering on the coated magnetic and metallic materials. The SI of Back wall was also

large because of reflection on multi-layer but smooth surface. On the contrary, the SIs of Slant walls and Front wall were small owing to diffraction and scattering, respectively.

The majority of cluster spreads and SI at 28 GHz were slightly smaller than that of 10 GHz, indicating that the channel tended to be more specular with less diffuse components as the frequency increases. This conclusion is also consistent with the previous studies [2], [13], [15]. It should also be noted that the slight difference of the half-power beamwidth of the UCA ($\sim$2.5 and $\sim$1 deg at 10 and 28 GHz) might also influenced the difference of AS between two bands.

These results implied two important points: First, the cluster spreads strongly depended on the number of layers and surfaces of the IOs, which was consistent with results reported in [14]. In contrast, the cluster SI was more related to the IO material and propagation mechanism. Second, the channel at 28 GHz was marginally more directive than that of 10 GHz as the majority of values were similar across two frequency bands.

TABLE II. Mean of cluster AS, DS, and SI and major mechanism

	AS [deg]		**DS [ns]**		**SI [dB]**		**Major mechanism/**
IO\freq [GHz]	10	28	10	28	10	28	**Number of layers**
Back wall	2.5	1.9	0.6	0.6	-3.8	-5.8	Reflection/Multi-layer
Window	1.7	1.2	0.4	0.2	-5.3	-6.5	Scattering/Single-layer
Slant left	2.8	1.7	0.8	0.5	-9.7	-9.5	Diffraction/Multi-layer
Front wall	2.9	1.2	0.7	0.2	-8.5	-9.4	Scattering/Multi-layer
Slant right	2.8	1	0.8	0.3	-7.4	-9.7	Diffraction/Multi-layer
Boards	3.9	3.5	1.1	0.9	-1.8	-1.3	Scattering/Multi-layer
Total	2.9	1.7	0.8	0.6	-6.9	-7.9	-

V. Conclusion

This paper discussed each IO/cluster SI and spreads characteristics at 10 and 28 GHz bands in the classroom environment. The results implied that the number of layers and surfaces of the IOs strongly influenced the cluster spreads. Moreover, the propagation mechanism and IO material had a great impact on cluster SI. Nevertheless, since the spreads were mostly small and SI was similar, the channels across two frequency bands exhibited highly directive characteristics and differences were marginal. Thus, similar modeling approaches may be utilized to model the channels. As the future work, detailed mechanism clarification will be done using PO.

Acknowledgment

This work was partly supported by JSPS KAKENHI Grant Number 16K18102 and 19K04369.

References

[1] T. S. Rappaport *et al.*, "Millimeter wave mobile communications for 5G cellular: It will work!" *IEEE Access*, vol. 1, pp. 335–349, 2013.

[2] W. Fan, I. Carton, J. Ø. Nielsen, K. Olesen, and G. F. Pedersen, "Measured wideband characteristics of indoor channels at centimetric and millimetric bands," *EURASIP J. Wireless Commun. and Networking*, vol. 2016, no. 1, p. 58, Feb 2016.

[3] J. Medbo, N. Seifi, and H. Asplund, "Frequency dependency of measured highly resolved directional propagation channel characteristics," in *Proc. 22th European Wireless Conf.*, May 2016, pp. 1–6.

[4] G. R. Maccartney, T. S. Rappaport, S. Sun, and S. Deng, "Indoor office wideband millimeter-wave propagation measurements and channel models at 28 and 73 GHz for ultra-dense 5G wireless networks," *IEEE Access*, vol. 3, pp. 2388–2424, 2015.

[5] K. Haneda, J. Järveläinen, A. Karttunen, M. Kyrö, and J. Putkonen, "A statistical spatio-temporal radio channel model for large indoor environments at 60 and 70 GHz," *IEEE Trans. Antennas Propagat.*, vol. 63, no. 6, pp. 2694–2704, June 2015.

[6] J. Huang *et al.*, "Multi-frequency mmwave massive MIMO channel measurements and characterization for 5G wireless communication systems," *IEEE J. Select. Areas Commun.*, vol. 35, no. 7, pp. 1591–1605, July 2017.

[7] G. Zhang *et al.*, "Millimeter-wave channel characterization at large hall scenario in the 10 and 28 GHz bands," in *2019 13th European Conference on Antennas and Propagation (EUCAP)*, March 2019, pp. 1–4.

[8] M. Peters *et al.*, "Measurement results and final mmMAGIC channel models," May 2017, deliverable D2.2.

[9] P. Hanpinitsak, K. Saito, J. Takada, M. Kim, and L. Materum, "Multipath clustering and cluster tracking for geometry-based stochastic channel modeling," *IEEE Transactions on Antennas and Propagation*, vol. 65, no. 11, pp. 6015–6028, Nov 2017.

[10] F. Fuschini *et al.*, "Analysis of in-room mm-wave propagation: Directional channel measurements and ray tracing simulations," *Journal of Infrared, Millimeter, and Terahertz Waves*, vol. 38, no. 6, pp. 727–744, Jun 2017.

[11] M. Kim, T. Iwata, K. Umeki, J. Takada, and S. Sasaki, "Indoor channel characteristics in atrium entrance hall environment at millimeter-wave band," in *2017 11th European Conference on Antennas and Propagation (EUCAP)*, March 2017, pp. 707–710.

[12] K. Wangchuk *et al.*, "Double directional millimeter wave propagation channel measurement and polarimetric cluster properties in outdoor urban pico-cell environment," *IEICE Trans. Commun.*, vol. E100-B, no. 7, pp. 1133–1144, Jul 2017.

[13] P. Hanpinitsak, K. Saito, W. Fan, J. Hejselbaek, J. Takada, and G. F. Pedersen, "Frequency characteristics of geometry-based clusters in indoor hall environment at shf bands," *IEEE Access*, vol. 7, pp. 75 420–75 433, 2019.

[14] ——, "Multi-path cluster characteristics in indoor environments at 28 GHz band," IEICE Technical Report, Tech. Rep. 120, AP2019-46, Jul. 2019.

[15] P. Hanpinitsak, K. Saito, W. Fan, J. Takada, and G. F. Pedersen, "Frequency characteristics of path loss and delay-angular profile of propagation channels in an indoor room environment in SHF bands," in *IEICE Technical Conf. Short Range Wireless Commun. (TCSRW)*, Mar 2017, pp. 1–6.

[16] G. Zhang *et al.*, "Experimental characterization of millimeter-wave indoor propagation channels at 28 GHz," *IEEE Access*, vol. 6, pp. 76 516–76 526, 2018.

[17] J. Hejselbaek, W. Fan, and G. F. Pedersen, "Ultrawideband VNA based channel sounding system for centimetre and millimetre wave bands," in *Proc. 27th Personal, Indoor, and Mobile Radio Commun. (PIMRC)*, Sept 2016, pp. 1–6.

[18] "Sz-2003000," http://www.ainfoinc.com/en/pro_pdf/new_products/antenna/Bi-Conical%20Antenna/tr_SZ-2003000-P.pdf, Ainfoinc, accessed: 2018-11-26.

[19] S. S. Zhekov, A. Tatomirescu, and G. F. Pedersen, "Modified biconical antenna for ultrawideband applications," in *Proc. 10th European Conf. Antennas and Propagation (EuCAP)*, April 2016, pp. 1–5.

[20] "Installation: A detailed insight into how to handle and mount plasterboard on a stud frame," https://mdbapi.knauf.com/v1/pdf_download.php?action=download&a=732006&c=a4ef762ba12191cc78c9a98ee1d17da4&p=g, Knauf, accessed: 2018-11-26.

[21] K. Haneda, J. Takada, and T. Kobayashi, "A parametric UWB propagation channel estimation and its performance validation in an anechoic chamber," *IEEE Trans. Microwave Theory Tech.*, vol. 54, no. 4, pp. 1802–1811, June 2006.

[22] J. Poutanen *et al.*, "Development of measurement-based ray tracer for multi-link double directional propagation parameters," in *Proc. 3rd European Conf. on Antennas and Propagation (EuCAP)*, March 2009, pp. 2622–2626.